Supplementary Information

Extremes meet: changeover between anti- and pro-oxidant activities of Cu-based nanozymes

Yuezhen He, [a] Yan Chen, [a] Xue Yang, [a] Chuncan Song, [a] Xianyong Shen, [a], Shirui Ma, [a] Jian sun, [a] Feng Gao *[a], and Lun Wang [a]

Anhui Province Key Laboratory of Biomedical Materials and Chemical Measurement, Key Laboratory of Functional Molecular Solids, Ministry of Education, Anhui Key Laboratory of Chemo/Biosensing, College of Chemistry and Materials Science, Anhui Normal University, Wuhu 241002, China.

Experimental section

Materials. Coppric chloride dihydrate, L-ascorbic acid, and *p*-terephthalic acid were purchased from Aladdin Scientific Corp (Shanghai, China). A SOD assay kit, a GPx assay kit and an •ON assay kit were bought from Beyotime Biotech. Inc. (Shanghai, China). Other reagents were purchased from Sinopharm Chemical Reagent Co. Ltd (Shanghai, China). All chemicals and reagents were used as received without further purification. Ultrapure water purified with a Millipore system (18.2 MΩ) was used throughout the experiments.

Instrumentation. The morphology of CuNCs nanozymes were recorded with a HT-7700 transmission electron microscope (Hitachi, Japan). High-resolution transmission electron microscope (HRTEM) was captured by using a Tecnai G220S-TWIN transmission electron microscope (FEI, USA). The fluorescence spectra were obtained by a Lumina Fluorescence Spectrometer (Thermo Fisher Scientific, Korea). UV−vis absorption spectra were carried out on a Hitachi UV-2910 spectrophotometer (Hitachi, Japan).

Synthesis of A-CuNCs. A-CuNCs were prepared by a one-step co-precipitation method[1, 2]. In a typical synthesis, 0.025 mmol $CuCl_2$ were dissolved in 30 mL deionized water and stirred with a magnetic stirrer for 10 minutes at room temperature. Then, aqueous L-ascorbic acid solution (100 mM, 5 mL) was slowly added to the above $CuCl_2$ solution, resulting in a light-yellow clarified solution. The mixture was called Solution A and was stirred for 3h. The solution was centrifuged at 15000 rpm for 25 min, and the precipitates were collected, washed thrice with ethanol. The obtained A-CuNCs were redispersed in ultrapure water and stored at 4 ^{o}C.

Synthesis of H-CuNCs. The procedure was the same as preparing A-CuNCs, except that Solution A was heated 80 ^{o}C for 3h.

Synthesis of B-CuNCs. The synthesis method was similar to that for A-CuNCs, except that the pH of Solution A was adjusted to 11 with NaOH (1M). The solution stirred for 3h at room temperature

to form a blue clarified solution.

OXD-like activity of CuNCs. The Oxide-like activity of three as-prepeared CuNCs was evaluated using TMB as a substrate. In a typical experiment, TMB (40 μL, 2 mg/mL), and CuNCs (400 μL) were added to a buffer (1.6 mL, pH=4.0) at 25℃. After incubating for 10 min, the UV-vis spectrums of the system at 652 nm were detected using a Hitachi UV-2910 spectrophotometer (Hitachi, Japan).

POD-like activity of CuNCs. The POD-like activity of three CuNCs were assayed using the oxidation of TMB in the presence of H_2O_2. In a typical experiment, TMB (40 μL, 2 mg/mL), CuNCs (400 μL), and H_2O_2 (40 μL, 10 mM) were added to a buffer (1520 μL, pH=4.0) at 25 °C. After mixing for 10 min, the absorbance of the system was measured at 652 nm. The steady-state kinetic assay of A-CuNCs were performed by varying the concentration of H_2O_2 (1.0, 2.0, 4.0, 8.0, and 16.0 mM) or TMB (0.2, 0.4, 0.8, 1.6, 3.2 and 6.4 mM) in the presence of g mL A-CuNCs.

CAT-like activity of CuNCs. The CAT-like activity of three CuNCs was evaluated determined by pTA fluorescence assay. In a typical experiment, pTA (40 μL, 5 mM), CuNCs (400 μL), and H_2O_2 (40 μL, 10 mM) were added to a buffer (1520 μL, pH=5.0) at 25℃. After mixing, the mixture was irradiated with a UV lamp of constant intensity for 15 min and the fluorescence intensity was measured at an excitation wavelength of 312 nm. The steady-state kinetic assay of A-CuNCs were performed by varying the concentration of H_2O_2 (2.0, 4.0, 6.0, 8.0, and 10.0 mM).

SOD-like activity of CuNCs. The SOD-like activity of three CuNCs was assessed using a SOD assay kit. A series of samples containing xanthine oxidase (0.5 U/mL) were placed in 10 mM PBS and incubated for 10 min at 37 °C. Different H-CuNCs (or B-CuNCs) (0, 20, 40, 60, 80, 100, 120 U/mL) were added and changes in absorbance values at A450 were recorded.

GPx-like activity of CuNCs. The GPx-like activity of H-CuNCs was assessed using a GPx assay kit. Glutathione peroxidase (GPx) can catalyze GSH to produce GSSG, while glutathione reductase (GR) can catalyze GSSG to produce GSH using NADPH, and the level of glutathione peroxidase (GPx) activity can be calculated by detecting the reduction of NADPH. The system was monitored by a UV spectrophotometer at 340 nm. The change in absorbance of the system was monitored by a UV spectrophotometer at 340 nm for 15min.

•ON scavenging activity of CuNCs. The •ON scavenging activity of three CuNCs was assessed using an •ON assay kit. The assay used Nitrate reductase to reduce Nitrate to Nitrite, followed by the classical Griess reagent to detect nitrite, which gave the final •ON content. The total amount of nitrate and nitrite was determined by the above method and the •ON content could be deduced.

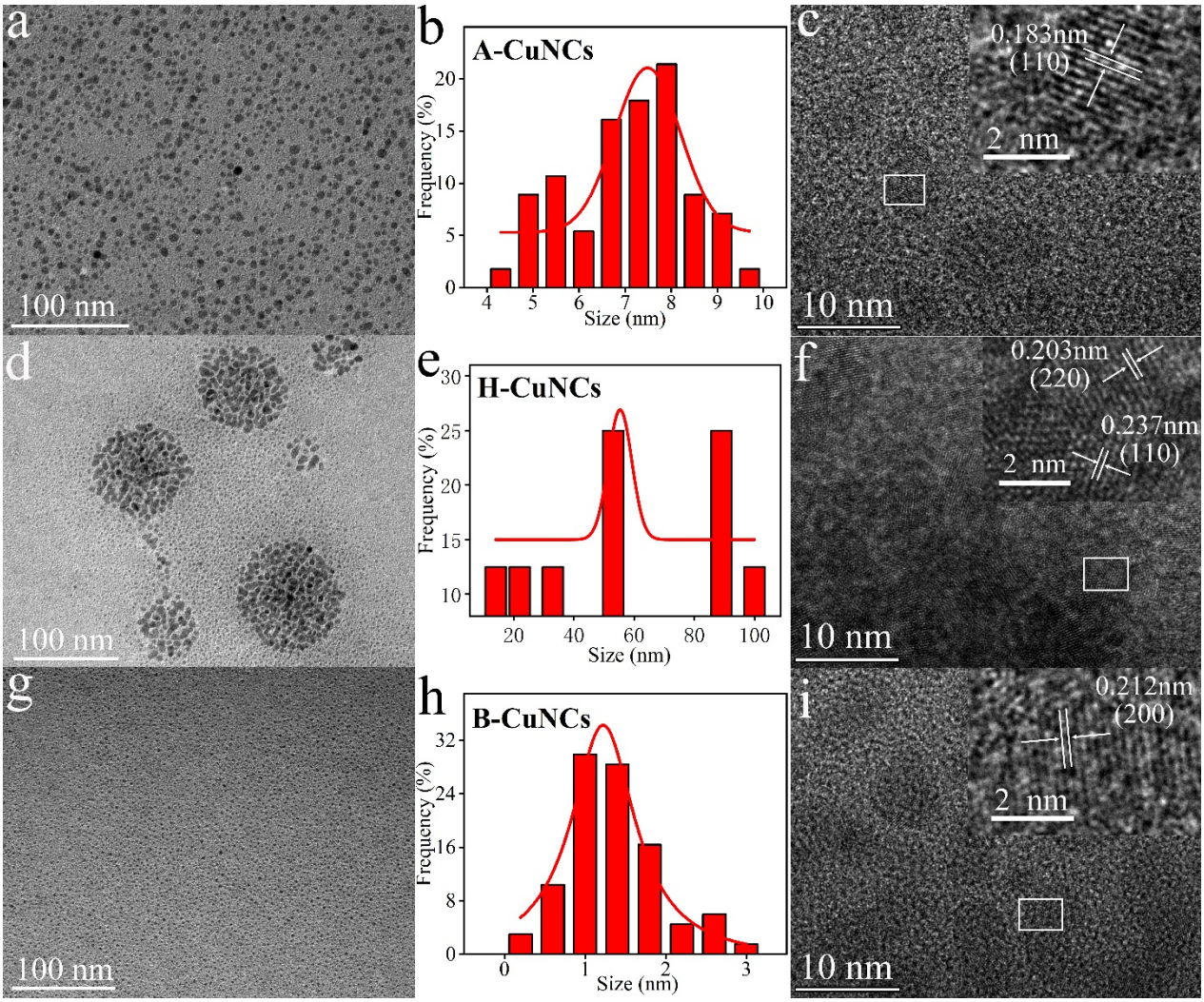

Fig. S1 Characterization of A-CuNCs, H-CuNCs and B-CuNCs. a, b and c TEM image, size distribution, and HR-TEM image for A-CuNCs; d, e and f TEM image, size distribution, and HR-TEM image for H-CuNCs; g, h, and i TEM image, size distribution, and HR-TEM image for B-CuNCs.

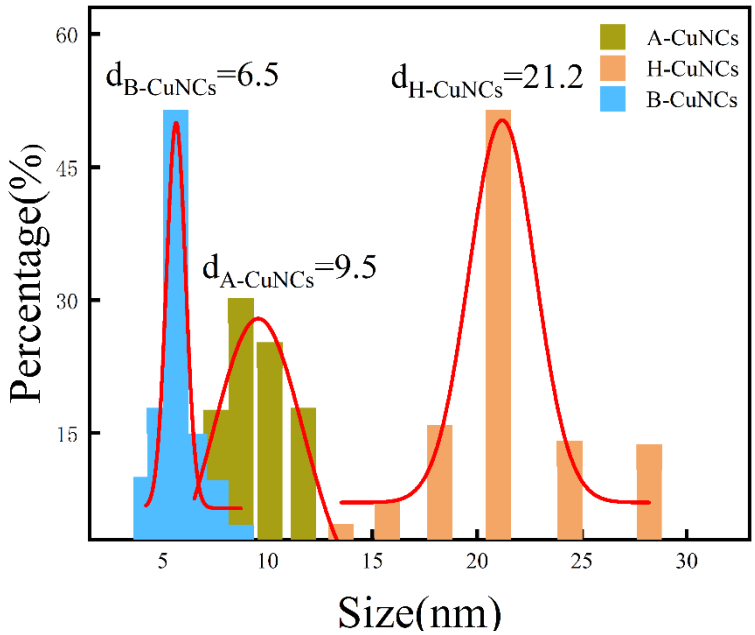

Fig. S2 hydrodynamic diameters of A-CuNCs, Ha-CuNCs and B-CuNCs by DLS

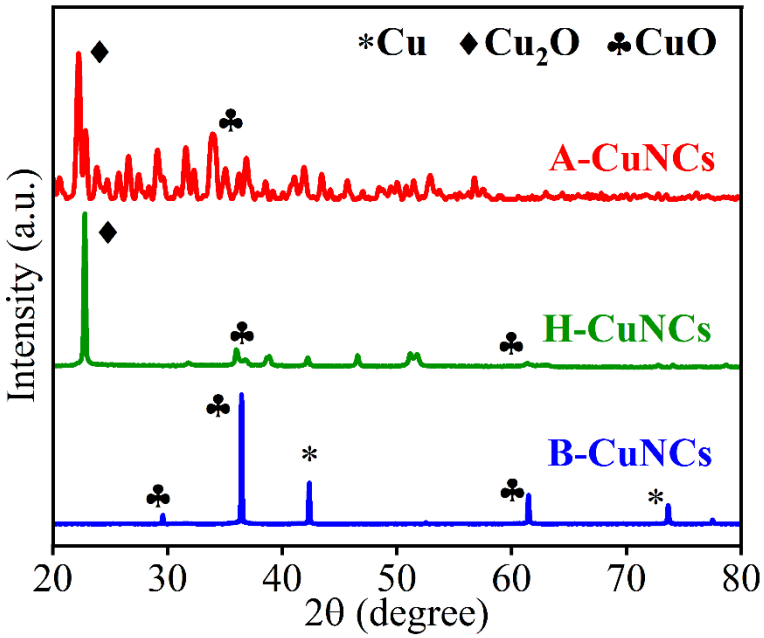

Fig. S3 XRD patterns of A-CuNCs, H-CuNCs and B-CuNCs. For A-CuNCs, the dominant peaks with 2θ= 22.9° were distributed on the (110) lattice planes of Cu(I), and the dominant peaks with 2θ= 36.3°were distributed on the (120) lattice planes of Cu(II) (JCPDS: 27-0297), showing that the A-CuNCs were a mixture of Cu(I) and Cu(II). The composition of H-CuNCs did not change significantly and still consisted of a mixture of Cu(I) and Cu(II). The dominant peaks of B-CuNCs at 2θ= 42.3°, 73.5° were distributed on the lattice planes of (200), (311) of Cu(0), and the lattice planes of B-CuNCs cuprous oxide (CuO) at 2θ= 29.6°(110), 36.4°(111), and 61.3° (220) had three small diffraction peaks, respectively (JCPDS: 05-0667), indicating that the B-CuNCs were a mixture of Cu(0) and Cu(II).

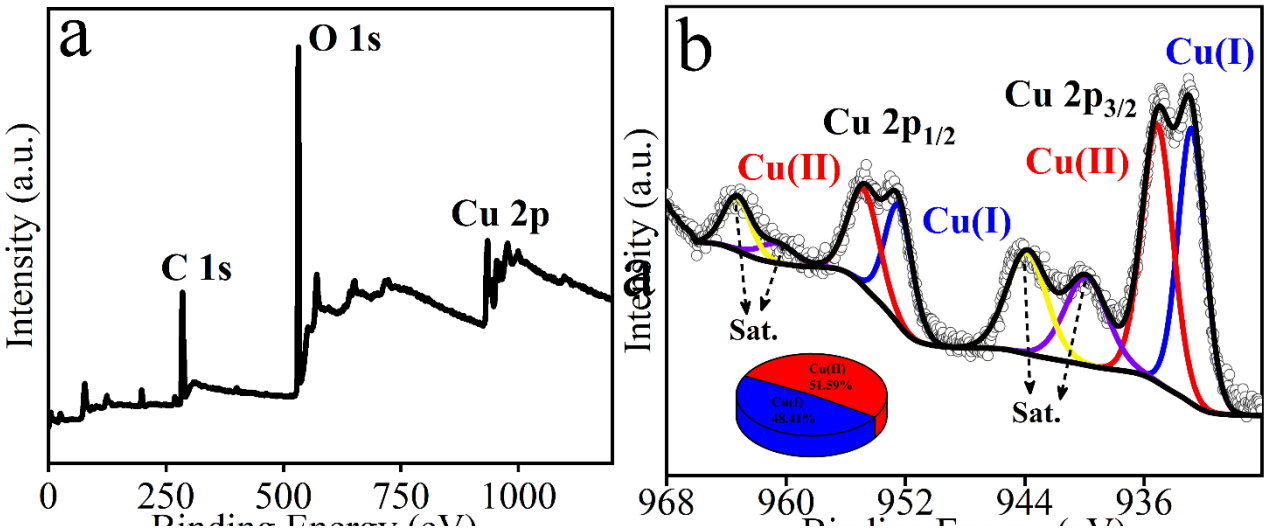

Fig. S4. (a) Full spectrum and (b) peak fitted Cu 2p XPS spectrum for A-CuNCs in XPS characterization. The peaks at 932.82 and 952.45 eV for A-CuNCs corresponded to Cu^{1+} $2p_{3/2}$ and Cu^{1+} $2p_{1/2}$ respectively; and two strong peaks at 935.11 and 954.78 eV corresponded to Cu^{2+} $2p_{3/2}$ and Cu^{2+} $2p_{1/2}$ respectively, indicating that the B-CuNCs were a mixture of Cu(I) and Cu(II) mixture, and the ratio of Cu(I) and Cu(II) can be derived from theoretical calculations as 48.4%:51.6%.

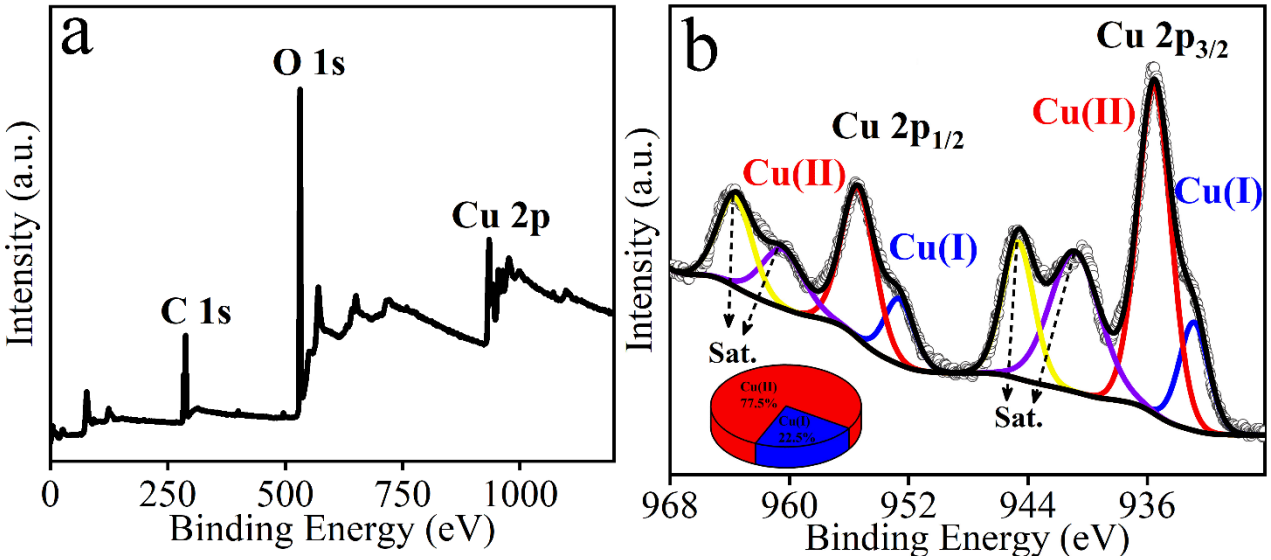

Fig. S5. (a) Full spectrum and (b) peak fitted Cu 2p XPS spectrum for H-CuNCs in XPS characterization. The peaks at 932.86 and 951.62 eV corresponded to Cu^{1+} $2p_{3/2}$ and Cu^{1+} $2p_{1/2}$ respectively; two strong peaks at 935.18 and 954.91 eV corresponded to Cu^{2+} $2p_{3/2}$ and Cu^{2+} $2p_{1/2}$ respectively, and the ratio of Cu(I) to Cu(II) is 22.5%:77.5%.

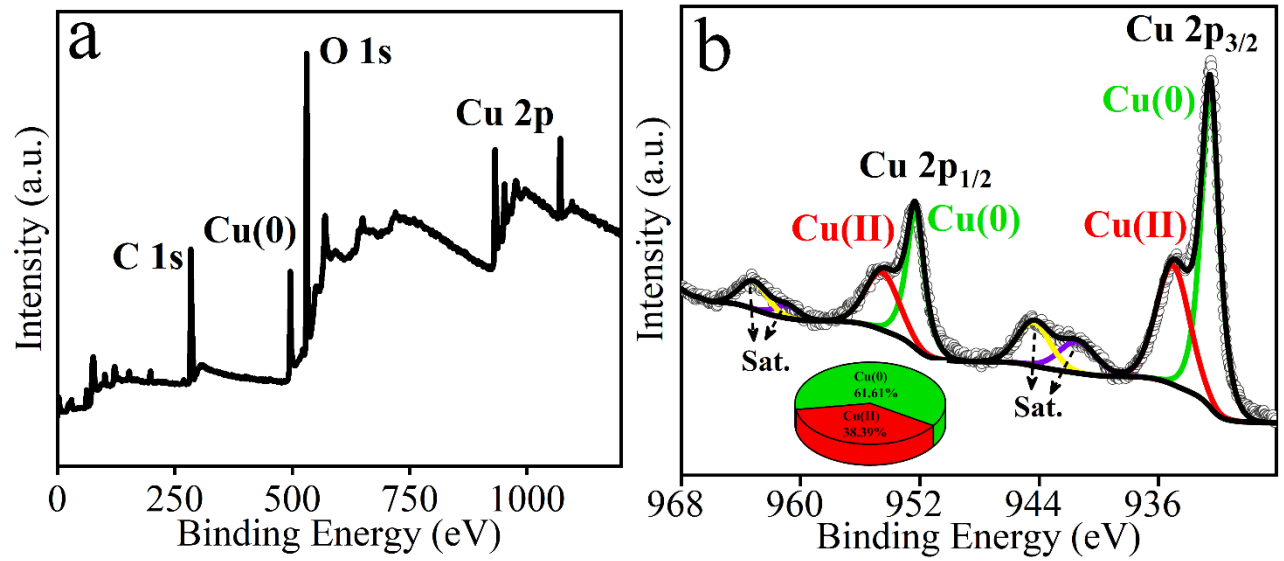

Fig. S6. (a) Full spectrum and (b) peak fitted Cu 2p XPS spectrum for B-CuNCs in XPS characterization. The peaks at 932.52 and 952.29 eV corresponded to Cu^{0} $2p_{3/2}$ and Cu^{0} $2p_{1/2}$ respectively, and the peaks at 934.02 and 954.52 eV corresponded to Cu^{2+} $2p_{3/2}$ and Cu^{2+} $2p_{1/2}$ respectively. while the Cu(0) to Cu(II) ratio of 61.6%:38.4% was obtained after theoretical calculations

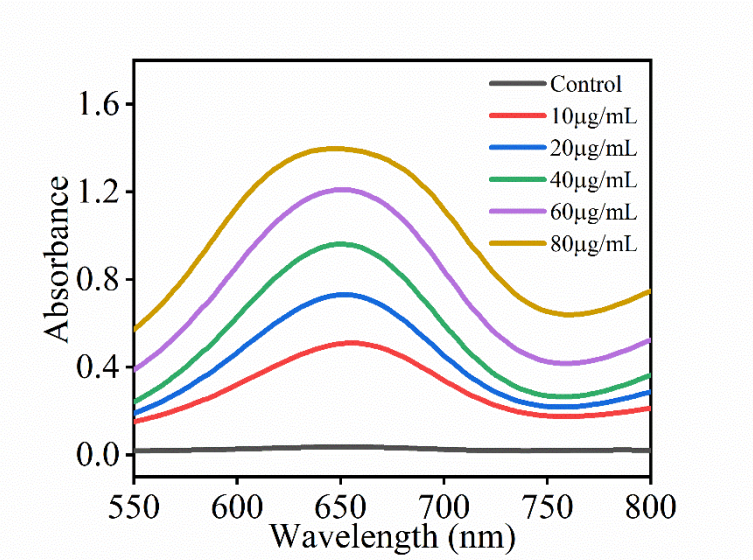

Fig. S7. UV-vis absorption spectra of TMB oxidation by O_2 in the presence of different concentration of A-CuNCs. The concentration of TMB and H_2O_2 is 50 μg/mL and 0.25 mM respectively.

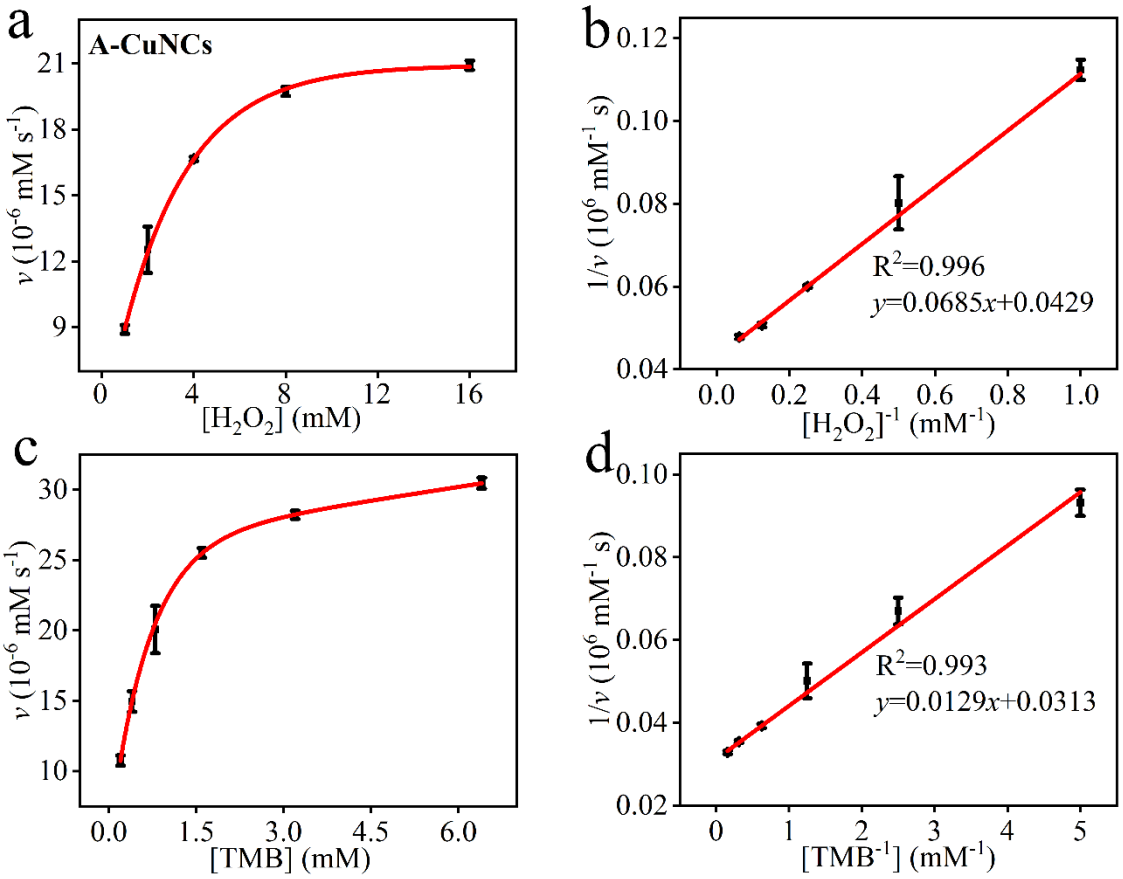

Fig. S8. POD-like catalytic activity of A-CuNCs. a Michaelis-Menten curve and b Lineweaver-Burk plotting for H_2O_2 catalyzed by A-CuNCs; c Michaelis-Menten curve and d Lineweaver-Burk for TMB catalyzed by A-CuNCs.

.

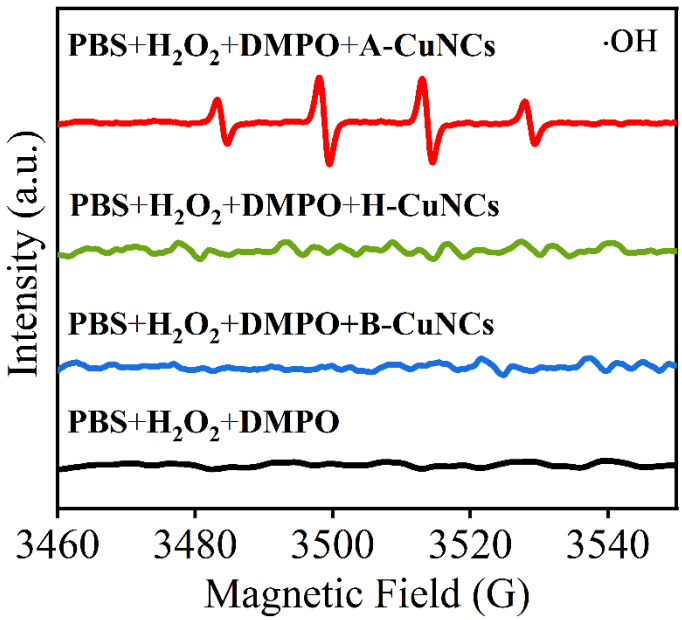

Fig. S9. EPR spectra of CuNCs for •OH characterization with 5,5-dimethyl-1-pyrroline-N-oxide (DMPO, 200 mM) as the spin-trap agent.

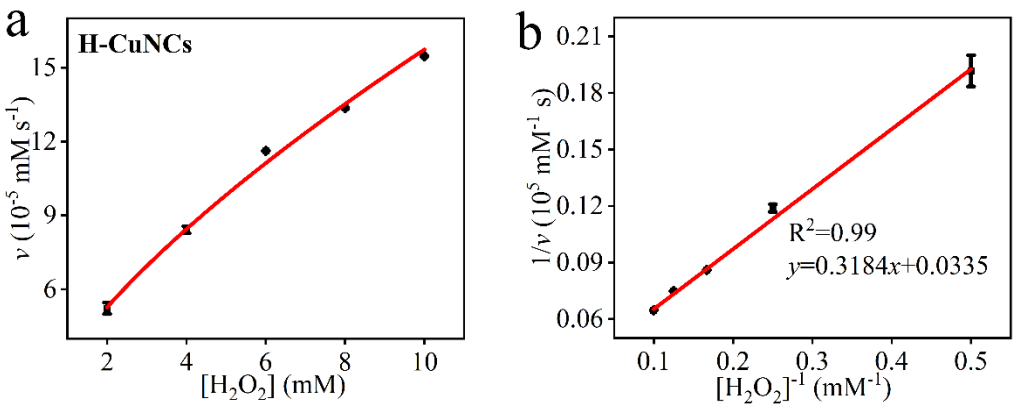

Fig. S10. Measurement of the Michaelis-Menten's constant K_m of H-CuNCs and the maximum reaction rate V_{max} of chemical kinetics.

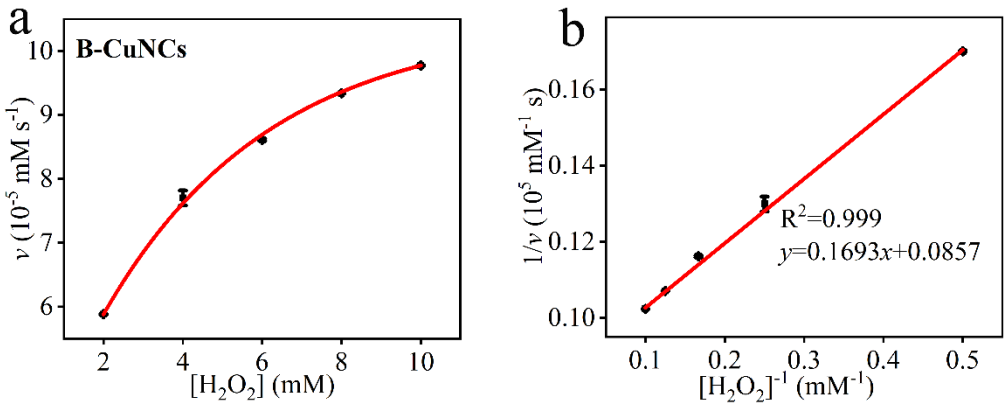

Fig. S11. Measurement of the Michaelis-Menten's constant K_m of B-CuNCs and the maximum reaction rate V_{max} of chemical kinetics.

Table S1. Comparisons of POD-like kinetic parameters of different nanocatalysts

Nanozymes	[E] (M)	Substrates	K_m (mM)	V_{max} (M s^{-1})	k_{cat}(s^{-1})	k_{cat}/ K_m ($M^{-1}s^{-1}$)	Ref
A-CuNCs	2.96×10^{-7}	H_2O_2	1.59	2.33×10^{-8}	0.0786	4.94	This
		TMB	0.414	3.21×10^{-8}	0.108	261	work
Cu_2O	6.54×10^{-6}	H_2O_2	0.444	4.83×10^{-8}	0.00739	-	3
Cu-N-C	2.68×10^{-6}	H_2O_2	19.94	2.0×10^{-7}	0.075	0.0038	4
		TMB	3.76	7.5×10^{-7}	0.2803	0.0746	
Fe-N-C	1.48×10^{-6}	H_2O_2	12.2	3.56×10^{-7}	0.24	19.67	5
		TMB	3.6	11.6×10^{-7}	0.78	216.67	

Table S2. Comparisons of CAT-like kinetic parameters of different nanocatalysts

Nanozymes	[E] (M)	K_m (mM)	V_{max} (M s^{-1})	k_{cat}(s^{-1})	k_{cat}/ K_m ($M^{-1}s^{-1}$)	Ref
H-CuNCs	2.96×10^{-7}	9.52	2.99×10^{-7}	1.01	106.1	This
B-CuNCs	2.96×10^{-7}	1.98	1.17×10^{-7}	0.39	197.0	work
$Cu_{5.4}O$	-	0.065	3.92×10^{-6}	-	-	1
MCCP	-	2.02	4.75×10^{-6}	3.49	-	6
Co_3O_4-MnO_2	1.2605×10^{-5}	104.73	1.75×10^{-4}	13.9	133	7
Co_3O_4	1.2605×10^{-5}	295.03	1.24×10^{-4}	9.84	33.7	

References

1. T. Liu, B. Xiao, F. Xiang, J. Tan, Z. Chen, X. Zhang, C. Wu, Z. Mao, G. Luo, X. Chen and J. Deng, *Nat. Commun.*, 2020, **11**. 2788
2. Y. He, M. Yin, J. Sun, J. Chen, K. Jiao, J. Wen, Y. Chen, B. Wang, F. Gao and L. Wang, *Cheml Commun.*, 2022, **58**, 2995-2998.
3. B. Yuan, H.-L. Chou and Y.-K. Peng, *Acs Appl. Mater. Interfaces*, 2022, **14**, 22728-22736.
4. Y. Wu, J. Wu, L. Jiao, W. Xu, H. Wang, X. Wei, W. Gu, G. Ren, N. Zhang, Q. Zhang, L. Huang, L. Gu and C. Zhu, *Anal. Chem.*, 2020, **92**, 3373-3379.
5. L. Jiao, W. Xu, H. Yan, Y. Wu, C. Liu, D. Du, Y. Lin and C. Zhu, *Anal. Chem.*, 2019, **91**, 11994-11999.
6. J. Zhou, D. Xu, G. Tian, Q. He, X. Zhang, J. Liao, L. Mei, L. Chen, L. Gao, L. Zhao, G. Yang, W. Yin, G. Nie and Y. Zhao, *J. Am. Chem. Soc.*, 2023, **145**, 4279-4293.
7. J. Huang, X. Jia, Y. Wang, Y. Qiao and X. Jiang, *Adv. Healthcare Mater.*, 2025, **14**, 2400401